Cell Research (2010) 20:138-153.

www.nature.com/cr

ORIGINAL ARTICLE

A GPCR/secretase complex regulates β- and γ-secretase specificity for Aβ production and contributes to AD pathogenesis

Lin Teng[1], Jian Zhao[1], Feifei Wang[2], Lan Ma[2], Gang Pei[1, 3]

[1]Laboratory of Molecular Cell Biology, Institute of Biochemistry and Cell Biology, Shanghai Institutes for Biological Sciences, Chinese Academy of Sciences; Graduate School of the Chinese Academy of Sciences, Shanghai 200031, China; [2]Pharmacology Research Center, Shanghai Medical School, Fudan University, Shanghai 200032, China; [3]School of Life Science and Technology, Tongji University, Shanghai 200092, China

Dysregulation of β-site APP-cleaving enzyme (BACE) and/or γ-secretase leads to anomalous production of amyloid-β peptide (Aβ) and contributes to the etiology of Alzheimer's disease (AD). Since these secretases mediate proteolytic processing of numerous proteins, little success has been achieved to treat AD by secretase inhibitors because of inevitable undesired side effects. Thus, it is of importance to unravel the regulatory mechanisms of these secretases. Here, we show that δ-opioid receptor (DOR) promotes the processing of Aβ precursor protein (APP) by BACE1 and γ-secretase, but not that of Notch, N-cadherin or APLP. Further investigation reveals that DOR forms a complex with BACE1 and γ-secretase, and activation of DOR mediates the co-endocytic sorting of the secretases/receptor complex for APP endoproteolysis. Dysfunction of the receptor retards the endocytosis of BACE1 and γ-secretase and thus the production of Aβ. Consistently, knockdown or antagonization of DOR reduces secretase activities and ameliorates Aβ pathology and Aβ-dependent behavioral deficits, but does not affect the processing of Notch, N-cadherin or APLP in AD model mice. Our study not only uncovers a molecular mechanism for the formation of a DOR/secretase complex that regulates the specificity of secretase for Aβ production but also suggests that intervention of either formation or trafficking of the GPCR/secretase complex could lead to a new strategy against AD, potentially with fewer side effects.

***Keywords*:** G protein-coupled receptor, Alzheimer's disease, BACE, γ-secretase, Notch

Cell Research (2010) **20**:138-153. doi: 10.1038/cr.2010.3; published online 12 January 2010

Introduction

Alzheimer's disease (AD) is the most common neurodegenerative disorder causing progressive memory loss and cognitive dysfunction [1]. Amyloid plaque composed of amyloid-β peptide (Aβ) in AD patient brains is one of the pathological hallmarks of the disease [2]. A large body of studies suggests that reduction of Aβ levels in the brain should be a promising therapeutic approach [3, 4]. Reduction of Aβ could conceivably be accomplished either by inhibiting its production or aggregation or by promoting its degradation and removal [5]. Aβ is derived from Aβ precursor protein (APP) after sequential β- and γ-endoproteolysis by β-site APP-cleaving enzyme 1 (BACE1) and γ-secretase complex, respectively [6-8]. BACE1 is the novel transmembrane aspartic protease that cleaves APP to form Aβ N-terminus and generate a C-terminal fragment, C99, as the substrate for γ-secretase [9]. Thus, BACE1 cleavage of APP is a prerequisite for γ-cleavage and is regarded as a rate-limiting step in the production of Aβ [10]. γ-Secretase is an intramembranous complex composed of presenilin-1 (PS1), PEN-2, nicastrin and APH-1, with PS1 constituting the active site [11]. Imprecise cleavage of C99 by γ-secretase produces Aβ variants, mainly Aβ40 and Aβ42 [12]. Conversely, cleavage of APP by α-secretase precludes the production

Correspondence: Gang Pei[a], Jian Zhao[b]
[a]E-mail: gpei@sibs.ac.cn
[b]E-mail: jzhao@sibs.ac.cn
Received 24 August 2009; revised 16 September 2009; accepted 17 September 2009; published online 12 January 2010

of the toxic Aβ peptide [13]. Accumulated Aβ can be removed by Aβ-degrading enzymes, such as neprilysin (NEP) [14], insulin-degrading enzyme (IDE) [15], endothelin-converting enzyme [16] and angiotensin-converting enzyme [17]. All these protease activities respond elaborately to diverse genetic and biochemical mediations. Dysregulation of either APP processing or Aβ clearance leads to anomalous Aβ deposition in brains, and contributes to the etiology of both familial and sporadic AD [18]. However, as the physiological roles of putative Aβ-degrading enzymes in Aβ clearance *in vivo* are still inconclusive, the β- and γ-secretases are thus regarded as key therapeutic targets so far. Nevertheless, in view of the multiple substrates of these secretases, designing drugs for specific inhibition of APP β- and γ-cleavage appears challenging.

Previous reports have shown that altered cell signaling, especially G protein-coupled receptor (GPCR) signaling, is related to abnormal Aβ production and AD pathogenesis [19-23]. We have previously reported that activation of β2-adrenergic receptor (β_2-AR) or δ-opioid receptor (DOR) directly enhances γ-secretase activity and accelerates Aβ production [23]. More recently, Thathiah *et al*. [24] have reported that expression of GPR3 led to increased formation and cell-surface localization of the mature γ-secretase complex in the absence of an effect on Notch processing. These findings, together with other studies, suggest that cellular membrane receptors, especially GPCRs, might be potential targets for modulating APP processing. Opioid receptors and opioid peptides are widely expressed in the central nervous system, including hippocampus and cortex, the brain regions crucial for cognition and vulnerable to AD. They play important roles in synaptic activation [25, 26], learning and memory [27, 28]. Administration of opioid antagonists has been found to significantly improve the memory of animals [27]; thus, in 1980s, the opioid antagonist naloxone was applied in a double-blinded placebo-controlled clinical study to test its potential effect on improving cognitive functioning in individuals with probable AD [29]. However, other studies have failed to support the efficacy of the nonselective antagonists naloxone or naltrexone in AD [30-32]. Given the distinct and even opposing roles of DOR, kappa-opioid receptor (KOR), and μ-opioid receptor (MOR) in modulating animal behaviors [33], the efficacy of selective opioid receptor antagonists for AD treatment needs to be further investigated. Recently, it has been reported that the levels of opioid receptors are differentially altered in distinct areas of postmortem brains of AD patients [34]. The levels of leu-enkephalin and dynorphin A (the endogenous opioid peptide for DOR and KOR, respectively) are also increased in the frontal cortex of patients with AD as compared to the control group [35]. Meilandt *et al*. [36] have shown that elevation of enkephalin levels contributes to the behavioral decline in a mouse model of AD. All these evidence suggests a possible role of the opioid system in AD pathology. Nevertheless, the mechanistic role of opioid receptors in Aβ pathology and AD pathogenesis was not explored so far.

In this study, we report that DOR forms a complex with BACE1 and γ-secretase, and activated DOR mediates the processing of APP but not that of Notch, N-cadherin or APLP. Mechanistic study reveals that activated DOR facilitates the endocytic sorting of the secretases for APP endoproteolysis. Dysfunction of the receptor retards the endocytosis of BACE1 and γ-secretase and thus the production of Aβ. Chronic treatment of transgenic AD model mice with an antagonist of DOR reduces endogenous BACE1 and γ-secretase activities, alleviates Aβ pathology and improves cognitive deficits in spatial reference memory. Reduction of BACE1 and γ-secretase activities by antagonizing DOR did not affect the processing of Notch, N-cadherin or APLP *in vivo*. Our study demonstrates the therapeutic potential of DOR antagonists for AD and also suggests that blockage of either the receptor-mediated secretase endocytosis or the association of the receptor with secretases should be potential strategies of targeting secretases specifically for Aβ production.

Results

Activation of DOR enhances BACE1 and γ-secretase activities specifically for Aβ production

We have previously reported that activation of DOR enhances γ-secretase activity *in vitro* [23]. Here, we first investigated whether activation of DOR specifically affects secretase activities for Aβ production. We overexpressed DOR in HEK293T cells and performed the fluorogenic substrate assay to directly evaluate the effect of DOR on secretase activities. HEK293T cells possess endogenous α-secretase, BACE1 and γ-secretase activities, and exhibit normal Aβ production. As shown in Figure 1A, 30 min after stimulation by [D-Ala^2, D-Leu^5]-enkephalin (DADLE), a specific DOR agonist, BACE1, and γ-secretase activities were enhanced to 143% and 156%, respectively, while the activity of α-secretase was not affected. This result indicates that activated DOR enhances BACE1 and γ-secretase activities in a relatively short time without altering the steady state level of secretases. Pretreatment with DOR selective antagonist naltrindole (NTI), on the other hand, blocked the enhancement of BACE1 and γ-secretase activities by

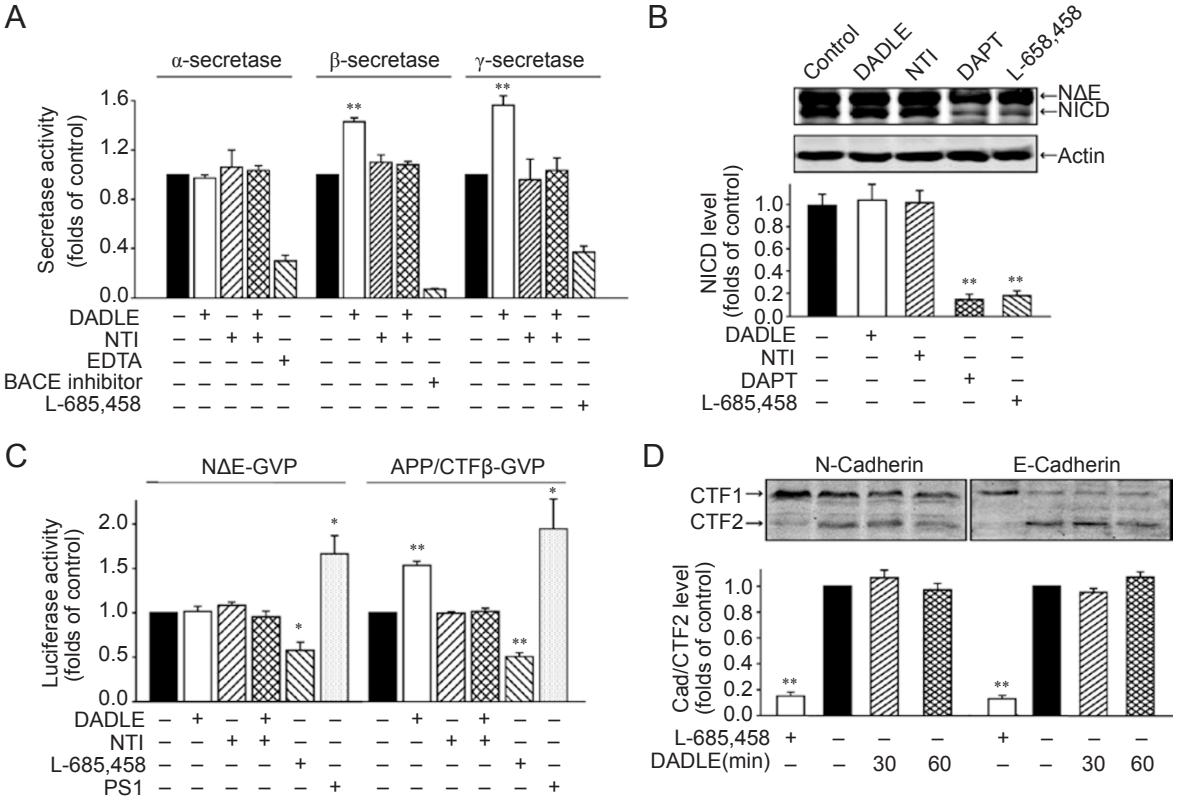

Figure 1 DOR activation specifically enhances BACE1 and γ-secretase activities for APP processing. **(A)** Activation of DOR-enhanced β- and γ-secretase activities in HEK293T cells. HEK293T cells stably overexpressing DOR were treated with 1 μM DADLE for 30 min in the presence or absence of NTI. The activities of α-, β- and γ-secretases were determined using fluorogenic substrate assay. EDTA (5 mM), BACE inhibitor (1 μM) or L-685,458 (1 μM) was applied as inhibitor of α-, β- or γ-secretase, respectively. **(B-D)** NTI or DADLE treatment does not affect Notch **(B**, **C)**, N-cadherin or E-cadherin **(D)** cleavage in HEK293T cells. HEK293T cells were transfected with DOR and myc-tagged NotchΔE. At 48 h after transfection, the cells were left untreated or treated with DAPT (1 μM), L-685,458 (1 μM), DADLE (1 μM) or NTI (1 μM) for 7 h, as indicated. Cell lysates were collected and subjected to immunoblots for NotchΔE and NICD. The representative images (upper) and densitometric analysis of the blots (bottom) were shown **(B)**. Alternatively, HEK293T cells stably overexpressing DOR were transiently transfected with the constructs carrying CMV-β-gal, MH100 and NotchΔE-GVP or APP/CTFβ-GVP together with or without PS1, and were treated as indicated for 12 h. Luciferase activity and β-galactosidase activity were measured **(C)**. HEK293T cells stably overexpressing DOR were treated as indicated. Membrane extracts were subjected to immunoblots for C-terminal fragment of N-cadherin or E-cadherin. The representative images and densitometric analysis results were shown **(D)**. Data from three independent experiments are presented as mean ± s.e.m. (Student's *t*-test; $*P < 0.05$, $**P < 0.01$).

DADLE, indicating that enhancement of secretase activities by DADLE depends on the activation of DOR.

The γ-secretase catalyses cleavage of many type-I integral membrane proteins and mediates the nuclear translocation of transmembrane receptors by proteolysis, most notably APP, Notch and cadherin [37]. We asked whether the enhancement of APP amyloidogenic cleavage by DADLE stimulation can be separated from the processing of Notch and cadherin. We overexpressed an ectodomain-shed form of Notch1 (NΔE) as described previously [38]. Notch ΔE lacks the ectodomain of the receptor and undergoes constitutive S3 cleavage by γ-secretase to generate the Notch intracellular domain (NICD) fragment in the absence of ligand [38]. As shown in Figure 1B, the production of NICD was blocked and NΔE was accumulated in the presence of either DAPT or L-685,458, two widely used γ-secretase inhibitors. However, neither NTI nor DADLE treatment altered the ratio of NICD and NΔE. The cell-based luciferase reporter gene assay using Gal4/VP16-tagged APP/CTFβ (APP/CTFβ-GVP) and Gal4/VP16-tagged NotchΔE (NΔE-GVP) [39] was further applied for quantification of APP/CTFβ and NotchΔE cleavage by γ-secretase. The cleavage of APP/CTFβ-GVP or NΔE-GVP by γ-secretase would release the transcription factor that activates luciferase expression, providing a quantitative measurement of APP/

CTFβ and NotchΔE γ-cleavage. As shown in Figure 1C, the luciferase activities were comparable in mock-treated, DADLE- or NTI-treated cells expressing NΔE-GVP, indicating that neither DADLE nor NTI treatment affects NotchΔE γ cleavage significantly. In contrast, activation of DOR leads to a robust increase of luciferase activity in cells expressing APP/CTFβ-GVP, showing a specific enhancement of APP γ-endoproteolysis. Moreover, Cad/CTF2 (cadherin C-terminal fragment) level was not affected by either NTI or DADLE treatment, but was reduced in the presence of L-685,458 (Figure 1D). These results indicate that in contrast to APP amyloidogenic processing that is efficiently increased in response to activation of DOR, proteolysis of Notch or N-cadherin by γ-secretase is not affected by DOR activation.

DOR activation leads to enrichment of BACE1 and γ-secretase in endocytic compartments

We have previously reported that β_2-AR associates with PS1 and that agonist-induced endocytosis of β_2-AR enhances trafficking of γ-secretase to late endosomes and increases Aβ production [23]. We hypothesized that a similar interaction-based mechanism might also apply here. We first performed immunoprecipitation experiments to verify the interaction of DOR with BACE1 and γ-secretase. As shown in Figure 2A, considerable amounts of HA-tagged BACE1 and endogenous PS1 were bound to the immunopurified FLAG-tagged DOR, while little ADAM10, a major α-secretase, was detected in the immunoprecipitates. Another GPCR, bradykinin B2 receptor (B2R), on the other hand, did not interact with PS1 or BACE1. This result suggests that DOR might form a complex with BACE1 and γ-secretase. To test this, we further performed a double immunoprecipitation assay. The protein complexes immunopurified by anti-FLAG matrixes from HEK293T cells expressing FLAG-tagged DOR and HA-tagged BACE1 were eluted using FLAG peptides and subsequently were immunoaffinity purified by anti-HA matrixes. As shown in Figure 2B, FLAG-tagged DOR and HA-tagged BACE1, as well as endogenous PS1 were clearly present in both the first-run and second-run immunoprecipitates (lanes 5 and 7), while little proteins were detected in the control mock immunoprecipitates (lanes 4 and 8). This result demonstrates that DOR, BACE1 and PS1 can form together in a complex.

GPCRs have been reported to be enriched in lipid raft and/or caveolae [40]. We investigated whether the association of DOR with PS1 and BACE1 is dependent on the integrity of lipid raft. We treated the cells with methy-β-cyclodextrin (MβCD), which disrupts lipid raft by removing cholesterol from the cell. Cells were then lysed, followed by immunoprecipitation. As shown in Figure 2C, the interaction between DOR and PS1 or BACE1 was significantly reduced by cholesterol depletion, indicating that the association is dependent on the integrity of lipid raft.

Next, we investigated whether the enhancement of BACE1 and γ-secretase activities by DADLE treatment involves agonist-induced receptor endocytosis. We used the membrane nonpenetrable reagent EZ-link Sulfo-NHS-LC-Biotin to specifically incorporate biotin into membrane proteins. The plasma membrane proteins can then be precipitated with streptavidin-agarose [41]. This approach has allowed us to track the membrane localization of BACE1 and PS1 after activation of DOR. As shown in Figure 2D and Supplementary information, Figure S1A, plasma membrane DOR, as well as BACE1 and PS1, were efficiently biotinylated and precipitated with streptavidin beads (lane 1). After DADLE stimulation, the levels of selectively biotinylated DOR, BACE1 and PS1 were reduced by ~34%, ~46% and ~30%, respectively. Based on these results, we hypothesized that activated DOR might direct the endocytosis of secretases. To test this, we performed confocal fluorescence time-lapse microscopy with HEK293T cells expressing fluorescently tagged BACE1 (RFP-BACE1) and PS1 (GFP-PS1) together with HA-tagged DOR. The subcellular location of RFP-BACE1 or GFP-PS1 is similar to that reported previously [42, 43]. Of interest, we detected a strong co-localization of RFP-BACE1 with GFP-PS1 in the presence of DOR (Figure 2E, second and third rows versus first row). Images recorded at 3-s intervals showed that right after DADLE stimulation, in cells expressing DOR, vesicles containing RFP-BACE1 and GFP-PS1 were endocytosed (Figure 2E, third row and Supplementary information, Video S1), strongly suggesting that activated DOR associates with BACE1 and γ-secretase, and mediates the endocytic sorting of these two proteases. Subcellular localization of secretases was then assessed in further details using immunofluorescence confocal microscopy. Cellular late endosomes and lysosomes (LEL) were marked by GFP-Rab7. We observed increased colocalization of HA-BACE1 or endogenous PS1 with GFP-Rab7 in LEL in response to activation of DOR by DADLE (Figure 2F). Together, these results suggest that DOR stimulation promotes the translocation of BACE1 and γ-secretase from plasma membrane to LEL.

Postendocytic sorting of activated DOR defines β- and γ-secretase trafficking and specifically enhances Aβ production

We asked whether different receptor endocytic sorting could coordinate with BACE1 and γ-secretase intracel-

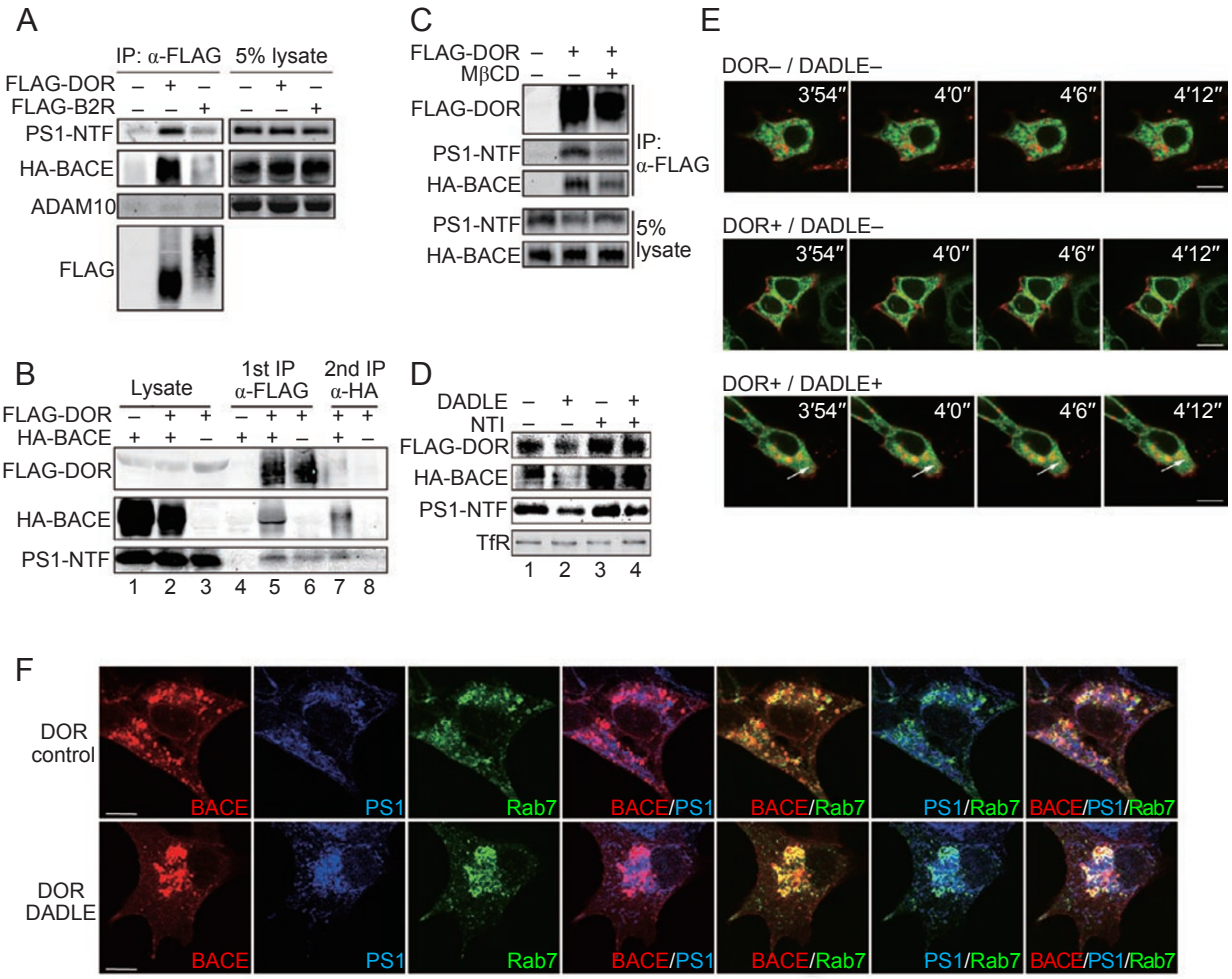

Figure 2 DOR couples with BACE1 and γ-secretase and enhances translocation of BACE1 and γ-secretase into endocytic compartments. **(A)** The association of DOR with BACE1 and PS1. Extracts of HEK293T cells overexpressing β-gal, 5′-FLAG-B2R or 5′-FLAG-DOR together with 3′-HA-BACE1, were subjected to immunoprecipitation with anti-FLAG M2 agarose. The cell lysates and the immunoprecipitated complexes were subjected to western blots for FLAG-DOR, ADAM10, HA-BACE1 and PS1-NTF. IP, immunoprecipitation. **(B)** DOR, BACE1 and PS1 are together in a complex. HEK293T cells overexpressing 3′-HA-BACE1 and 5′-FLAG-DOR were lysed and immunoprecipitated with anti-FLAG M2 agarose. The immunoprecipitated protein complex bound to the beads was eluted with FLAG peptide and subjected to second immunoprecipitation using anti-HA agarose. The eluates from the first and second immunoprecipitation and cell lysates were separated by SDS-PAGE and blotted using the antibodies against FLAG, HA and PS1-NTF. **(C)** The association of DOR with PS1 and BACE1 is dependent on lipid raft. HEK293T cells overexpressing β-gal or 5′-FLAG-DOR together with 3′-HA-BACE1 were left untreated or treated with MβCD (10 mM for 1 h), and then were subjected to immunoprecipitation with anti-FLAG M2 agarose. The cell lysates and the immunoprecipitated complexes were subjected to western blots for FLAG-DOR, HA-BACE1 and PS1-NTF. **(D)** The decreased levels of DOR, BACE1 and PS1 on the plasma membrane after DADLE treatment. HEK293T cells overexpressing 5′-FLAG-DOR and 3′-HA-BACE1 were stimulated with 1 μM DADLE for 30 min in the presence or absence of NTI, respectively. The proteins on the plasma membrane were labeled by EZ-link Sulfo-NHS-LC-Biotin, collected by streptavidin-agarose and detected on immunoblots. Transferrin receptor (TfR) levels were monitored in parallel as a loading control. The representative images were shown. **(E)** Time-lapse analysis of β- and γ-secretases subcellular localization after DOR activation. HEK293T cells were transfected with RFP-BACE1 and GFP-PS1 with or without DOR. At 42 h after transfection, cells were left untreated or were treated with 1 μM DADLE. Images were acquired every 3 s using a Ultraview laser spinning disc confocal microscope (Perkin Elmer). Arrows indicate the endocytosis of a typical vesicle containing both RFP-BACE1 and GFP-PS1. Scale bars, 10 μm. **(F)** Immunofluorescent confocal microscopy of BACE1 and PS1 after DOR activation. HEK293 cells transiently expressing GFP-Rab7 and HA-BACE1 together with 5′-FLAG-DOR were treated with or without 1 μM DADLE for 30 min. The cells were then fixed and stained with primary antibodies against PS1 and HA followed by CY3- or CY5-conjugated secondary antibodies. Representative images showed the localization of Rab7 (green), BACE1 (red) and PS1 (blue). Scale bars, 10 μm.

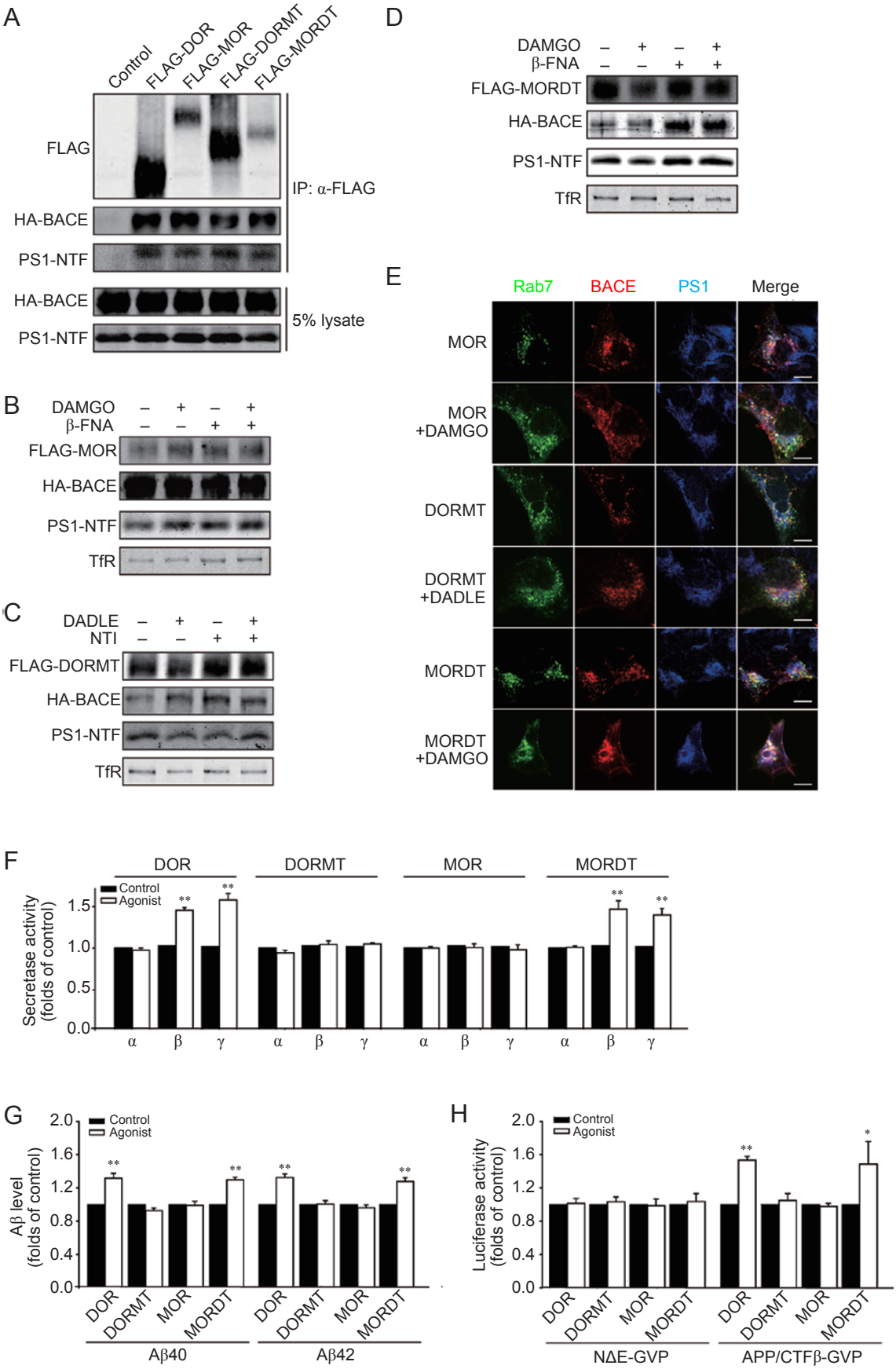
A
Control
FLAG-DOR
FLAG-MOR
FLAG-DORMT
FLAG-MORDT
FLAG
IP: α-FLAG
HA-BACE
PS1-NTF
HA-BACE
PS1-NTF
5% lysate
B
DAMGO – + – +
β-FNA – – + +
FLAG-MOR
HA-BACE
PS1-NTF
TfR
C
DADLE – + – +
NTI – – + +
FLAG-DORMT
HA-BACE
PS1-NTF
TfR
D
DAMGO – + – +
β-FNA – – + +
FLAG-MORDT
HA-BACE
PS1-NTF
TfR
E
Rab7
BACE
PS1
Merge
MOR
MOR +DAMGO
DORMT
DORMT +DADLE
MORDT
MORDT +DAMGO
F
DOR
DORMT
MOR
MORDT
Control
Agonist
Secretase activity (folds of control)
1.5
1.0
0.5
0.0
α β γ α β γ α β γ α β γ
G
Control
Agonist
Aβ level (folds of control)
2.0
1.6
1.2
0.8
0.4
0.0
DOR DORMT MOR MORDT DOR DORMT MOR MORDT
Aβ40
Aβ42
H
Control
Agonist
Luciferase activity (folds of control)
2.0
1.6
1.2
0.8
0.4
0.0
DOR DORMT MOR MORDT DOR DORMT MOR MORDT
NΔE-GVP
APP/CTFβ-GVP

lular trafficking. It has been reported that binding of GPCR-associated sorting protein (GASP) to the DOR cytoplasmic tail modulates lysosomal sorting of activated DOR [44]. On the contrary, MOR is uncapable of interacting with GASP and rapidly recycles back to the plasma membrane after activation [45]. Exchanging the cytoplasmic tail of DOR with that of MOR swapped the postendocytic sorting profiles of the receptors [44, 46]. Therefore, we used these chimeric receptors (DORMT, DOR with the C-terminal tail of MOR, and MORDT, MOR with the C-terminal tail of DOR) to test whether different endocytic and postendocytic behaviors of the receptors are linked to the regulation of BACE1 and γ-secretase. The interaction of the receptors with either BACE1 or PS1 was not affected by exchanging the cytoplasmic tails (Figure 3A). We then performed the membrane protein precipitation assay. We found that activation of MOR by its specific agonist [D-Ala^2,NMePhe^4,Gly(ol)^5]enkephalin (DAMGO) did not affect the levels of the receptor, BACE1 and PS1, on membrane (Figure 3B and Supplementary information, Figure S1B). Interestingly, following the activation of the chimeric receptor DORMT by DADLE, the level of BACE1 or PS1 on cell membrane was not significantly different from that in the untreated control cells (Figure 3C and Supplementary information, Figure S1C), indicating that unlike wild-type (WT) DOR, DORMT could not promote the translocation of BACE1 and γ-secretase from plasma membrane to LEL. In contrast, activation of MORDT by DAMGO led to decreased BACE1 and PS1 membrane localization, as did WT DOR (Figure 3D and Supplementary information, Figure S1D), indicating that postendocytic sorting of the receptor is critical for mediation of BACE1 and PS1 subcellular translocation. Further, confocal microscopy images showing that activated MORDT targeted both BACE1 and PS1 to LEL (lower two rows), as did WT DOR, confirmed the endocytic trafficking of BACE1 and PS1 after MORDT activation (Figure 3E). Consistently, activation of MORDT by DAMGO enhanced the activities of BACE1 and γ-secretase similar to activated DOR, whereas neither activation of DORMT by DADLE nor stimulation of MOR by DAMGO affected the secretase activities (Figure 3F). We also monitored the Aβ production and observed an increase of Aβ40 and Aβ42 levels after activation of DOR and MORDT (Figure 3G). We further analyzed the cleavage of APP/CTFβ or NotchΔE by γ-secretase in the presence of the chimeric receptor MORDT. As shown in Figure 3H, while the luciferase activities were comparable in cells expressing NΔE-GVP with or without agonists, cleavage of APP was specifically enhanced by cognate agonist treatment, indicating that postendocytic sorting of the membrane receptor regulates the specificity of BACE1- and γ-secretase-mediated proteolysis for different substrates.

Antagonization of DOR by NTI mitigates AD-like pathology in mice

Based on these results, we hypothesized that blockage of DOR or MOR might differently affect Aβ-dependent pathogenesis and behavioral deficits *in vivo*. To test this, we chronically administered either NTI or β-funaltrexamine (β-FNA) to APP/PS double-transgenic mice. NTI and β-FNA are highly selective and potent

Figure 3 Postendocytic sorting of activated DOR defines BACE1 and γ-secretase trafficking and specifically enhances Aβ production. **(A)** Association of the receptors with BACE1 and PS1. Extracts of HEK293T cells overexpressing 3′-HA-BACE1 together with 5′-FLAG-DOR, 5′-FLAG-MOR, 5′-FLAG-DORMT or 5′-FLAG-MORDT were subjected to immunoprecipitation with anti-FLAG M2 agarose. Lysates as well as the immunoprecipitated complexes were subjected to western blots for the receptors (FLAG), HA-BACE1 and PS1-NTF, respectively. **(B-D)** Activated MORDT **(D)**, but not MOR **(B)** or DORMT **(C)**, mediates endocytosis of BACE1 and PS1. HEK293T cells overexpressing 5′-FLAG-MOR, 5′-FLAG-DORMT or 5′-FLAG-MORDT were stimulated with their specific ligands for 30 min as indicated. The proteins on the membrane were labeled by EZ-link Sulfo-NHS-LC-Biotin, collected by streptavidin-agarose and detected on immunoblots. The representative images were shown. **(E)** Immunofluorescent confocal microscopy of BACE1 and PS1 after activation of MOR, DORMT or MORDT. HEK293 cells transiently expressing GFP-Rab7 and HA-BACE1 together with 5′-FLAG-MOR, 5′-FLAG-DORMT or 5′-FLAG-MORDT were treated with indicated agonists (1 μM for 30 min). The cells were then fixed and stained with primary antibodies against PS1 and HA. Representative images showed the localization of Rab7 (green), BACE1 (red) and PS1 (blue). Scale bars, 10 μm. Secretase activities **(F)** and Aβ production **(G)** in cells after activation of DOR, DORMT, MOR or MORDT. HEK293T cells stably overexpressing APPswe were transfected with 5′-FLAG-DOR, 5′-FLAG-DORMT, 5′-FLAG-MOR or 5′-FLAG-MORDT and were stimulated with indicated agonists (1 μM, 30 min for secretase activity or 7 h for Aβ production). The activities of α-, β- and γ-secretases were determined using fluorogenic substrate assay. The levels of Aβ40 and Aβ42 in the conditioned medium were measured by ELISA. **(H)** The cleavage of APP and Notch in cells after activation of DOR, DORMT, MOR or MORDT. HEK293T cells were transfected with the indicated receptor and the constructs carrying CMV-β-gal, MH100 and NotchΔE-GVP or APP/CTFβ-GVP, treated and measured for the luciferase activity and β-galactosidase activity. Data are presented as mean ± s.e.m. and are presented as folds of control untreated sample. (Student's *t*-test; **P* < 0.05, ***P* < 0.01).

non-peptide antagonists for DOR and MOR, respectively [47, 48]. Both NTI and β-FNA have good blood-brain-barrier permeability and bioavailability [49, 50]. Chronic administration of either NTI or β-FNA to animals leads to no obvious toxic side effects as reported [51]. APP/PS double-transgenic mice coexpress a chimeric mouse/human APP Swedish mutant (APPswe) and a mutant human PS1 (PS1ΔE9) [52]. These transgenic mice display an aggressive onset of age-dependent neuritic Aβ deposition in the cortex and hippocampus, and begin to show memory deficits at the age of 6 months [53, 54]. Drug administration began prophylactically at 4 months of age (that is, about 2 months before the onset of phenotype). Gender- and age-matched APP/PS transgenic mice and their transgene-negative (WT) littermates were administered with NTI (5 mg/kg per day), β-FNA (20 mg/kg per day) or vehicle by oral gavage once per day for 60 days. At the doses we chose, both NTI and β-FNA were reported to effectively attenuate a variety of behaviors that are mediated by DOR or MOR, respectively [55-58]. The drug administration caused no obvious weight loss or other adverse changes. After drug administration, we assayed spatial learning and reference memory of these mice in the Morris water maze. NTI or β-FNA treatment did not affect mouse motor function, as assessed by the swimming speed (Supplementary information, Figure S2A). During visible platform testing (learning phase), all mice showed similar learning latencies (Supplementary Figure S2B), indicating that NTI or β-FNA treatment had little effect on the vision, motor ability or motivation of the mice. However, as shown in Figure 4A, during hidden platform testing, APP/PS mice showed a significantly slower learning rate compared with the transgene-negative littermates ($P = 0.007$), indicating consistent learning and memory deficits of APP/PS mice, as reported previously [59]. Interestingly, chronic NTI treatment, but not β-FNA treatment, reversed the spatial learning and memory impairment of APP/PS mice ($P < 0.001$ APP/PS NTI-treated mice versus APP/PS control mice; $P = 0.507$ APP/PS NTI-treated mice versus transgene-negative mice; $P = 0.309$ APP/PS β-FNA-treated mice versus APP/PS control mice, Figure 4A). To assess reference memory at the end of learning, we administered a probe trial 24 h after the last day of acquisition. In comparison with the vehicle-treated or β-FNA-treated APP/PS mice, the NTI-treated APP/PS mice passed the position of platform more often ($P = 0.031$ versus APP/PS control mice, Figure 4B) and spent more time in the quadrant where the platform used to be ($P = 0.027$ versus APP/PS control mice, Supplementary information, Figure S2C). There was no detectable difference of behavior between vehicle-treated APP/PS transgenic mice and untreated APP/PS transgenic mice (data not shown). These results indicate that administration of NTI attenuates the spatial learning and reference memory deficiency in APP/PS transgenic AD model mice.

After the behavioral tests, the APP/PS transgenic mice were sacrificed and their Aβ and β-amyloid pathology were assessed. APP/PS mice showed typical elevated Aβ level and detectable thioflavin S-positive β-amyloid deposits at 6.5 months of age, which were markedly reduced in cortical areas by 51% in NTI-treated APP/PS mice ($P = 0.042$ versus APP/PS control mice) but not in β-FNA-treated APP/PS mice (Figure 4C). Immunofluorescent staining of Aβ in these sections also demonstrated an obvious reduction (58%) of Aβ deposits by NTI treatment ($P = 0.040$ versus APP/PS control mice, Figure 4C). We then used sandwich ELISA to quantify Aβ levels in these mice. The tissue was first extracted by detergent (SDS fraction) and the nonsoluble pellet was further extracted with formic acid (FA fraction). ELISA analysis showed high levels of Aβ in both fractions from hippocampus or cortex of 6.5 month-old APP/PS transgenic mice, whereas WT littermates had undetectable Aβ levels. We observed a consistent reduction of the hippocampal Aβ40 and Aβ42 levels by NTI treatment (75% reduction for Aβ40 and 43% reduction for Aβ42 in the detergent-soluble fraction (Figure 4D) and 80% reduction for Aβ40 and 71% reduction for Aβ42 in the formic acid-extractable fraction (Supplementary information, Figure S2D)). We also observed a similar reduction of cortical Aβ level after NTI treatment (Figure 4D and Supplementary information, Figure S2D). These results indicate that blockade of DOR by NTI but not that of MOR by β-FNA reduces both Aβ and β-amyloid pathology in these transgenic mice.

Amyloid plaques are invariably surrounded by activated inflammatory cells such as astrocytes and microglia, as is common in AD patient brains and transgenic AD model mice [60, 61]. We observed that clusters of reactive astrocytes stained with glial fibrillary acidic protein (GFAP) were visible surrounding the amyloid plaques (Figure 4E). Activated microglia strongly immunoreactive to anti-CD11b antibodies were also observed in close association with the amyloid plaques (Figure 4E). We noted substantial reductions of activated GFAP-positive astrocytes and CD11b-positive microglia in NTI-treated mice (Figure 4E). These results demonstrate that blockage of DOR by NTI significantly reduces AD-like pathogenesis in mice.

Blockade of DOR by NTI specifically reduces BACE1 and γ-secretase activities for Aβ production

Reduction of amyloidosis in NTI-treated APP/PS

A
Escape latency (s)
Blocks (hidden)
WT
APP/PS
APP/PS+NTI
APP/PS+β-FNA
B
Number crossing over platform
WT
APP/PS
APP/PS+NTI
APP/PS+β-FNA
C
Vehicle
NTI
β-FNA
Thiofla-vin S
Aβ
Aβ immuno-reactivity area (10³ arbitrary unit)
Plaque area (10³ arbitrary unit)
D
Hippocampal Aβ level (ng/g wet weight)
Aβ40
Aβ42
E
GFAP
CD11b
GFAP immuno-reactivity area (10³ arbitrary unit)
CD11b-positive microglia (profiles/section)
F
APP level (folds of control)
FL
CTFβ
CTFα
G
Secretase activity (folds of control)
α
β
γ
Relative protein level (folds of control)
NICD
N-Cad/CTF1
APL-Pi-CTF
H
Vehicle
NTI
β-FNA
NICD
N-Cad/CTF1
APL1-FL
APLP1-CTF
Actin

mouse brain could be due to reduced amyloidogenic APP metabolism or increased Aβ clearance. The results of fluorogenic substrate assay showed that the activities of Aβ-degrading enzymes, NEP and IDE, were not affected by administration of either NTI or β-FNA (Supplementary information, Figure S2E). We next investigated steady-state APP metabolism by analyzing the abundance of amyloidogenic (CTFβ, C99) and nonamyloidogenic (CTFα, C83) carboxyl terminal APP fragments. We found that the levels of C99 and C83 were elevated in NTI-treated APP/PS mice, whereas the levels of full-length APP were not altered (Supplementary information, Figure S2F and Figure 4F). This observation supported our hypothesis that the reduction of Aβ levels in NTI-treated APP/PS mice is caused by the alteration of secretase activities but not by changes of APP expression levels or Aβ clearance. Further fluorogenic substrate analysis showed that the activities of BACE1 and γ-secretase were significantly reduced upon administration of NTI, whereas no detectable changes of α-secretase activity were observed (Figure 4G). These results suggest that blockage of DOR, but not MOR, downregulates BACE1 and γ-secretase activities and leads to reduced Aβ-related pathology.

We further assessed whether NTI treatment affects proteolysis of other proteins by either BACE1 or γ-secretase. To this end, the levels of NICD, N-cadherin C-terminal fragment (N-Cad/CTF1) and APLP1 and its C-terminal fragment (APLP1-CTF) were monitored. We found that NICD levels were indistinguishable among different groups of treated mice (Figure 4H). Likewise, the level of N-Cad/CTF1, a direct substrate for γ-secretase generated by metalloprotease cleavage of N-cadherin, was also not affected (Figure 4H). Two known APP-like proteins, APLP1 and APLP2, undergo proteolysis by α-, β- and γ-secretase, similar to that of APP [62]. We found no discernible difference in either APLP1-CTF or APLP1-FL levels in NTI-, β-FNA- and vehicle-treated mice (Figure 4H), indicating that the processing of APLP1 was not affected by NTI treatment either. Together, these results indicate that blockage of DOR by NTI specifically reduces amyloidogenic APP cleavage by BACE1 and γ-secretase *in vivo*, but spares Notch, N-cadherin or APLP1 processing.

Knockdown of DOR retards Aβ accumulation and amyloid plaque formation in mice

Finally, we tested whether DOR contributes to the pathogenesis of AD *in vivo*. We used the lentiviral system to knock down the endogenous DOR1 in hippocampus of TgCRND8 mice, a transgenic AD mouse model. These mice carry a human mutant amyloid precursor protein transgene (APP_{695}K670N, M671L and V717F), and show progressive cognitive deficiency and detectable amyloid plaques from the age of 3 months [63]. We injected lentiviral vectors carrying DOR siRNA (lenti-siDOR) into the right side and control vectors carrying scrambled oligos into the left side of the hippocampus of 3-month-old TgCRND8 mice. Fluorescent images of coexpressed GFP indicated the distribution of these lentiviral vectors. At 2 months after injection, we observed expression of GFP throughout the dentate gyrus with abundant distribution in the cell bodies and dendrites (Figure 5A). Both lentiviral vectors were expressed at comparable levels in the bilateral hippocampi. Quantitative PCR coupled

Figure 4 Antagonizing of DOR retards Aβ accumulation and ameliorates AD-like pathology in mice. **(A)** NTI treatment attenuates the deficiency of APP/PS transgenic mice in spatial learning. APP/PS transgenic mice were trained and tested on the spatial memory version of the Morris water maze. During hidden platform training, the APP/PS mice showed a slower learning curve compared with WT littermates (F (1 115) = 8.780, P = 0.007). This impairment in spatial learning was reversed by NTI treatment (APP/PS versus APP/PS+NTI; F(1 120) = 13.103, P < 0.001). The significant difference was determined by two-way RMANOVA. **(B)** Performance of APP/PS transgenic mice in probe trial of Morris water maze. The mice were given a probe trial 24 h after the last training trial. Number crossing over platform and representative search paths were shown. The black dot showed the position where the platform used to be. n = 8-17 per group. **(C)** Thioflavin S-positive plaque and 6E10-positive Aβ deposits. Representative images (left) and morphometric analysis (right) were shown. Scale bars, 50 μm. **(D)** The Aβ level in detergent extracts (SDS) from hippocampus (upper) and cortex (bottom). Detergent extracts from hippocampus or cortex of the mice were prepared and subjected to sandwich ELISA assay for Aβ40 and Aβ42. **(E)** Astrocytes and microglia. The brain sections were probed using antibody to GFAP and antibody to CD11b. Representative images (upper) and morphometric analysis (bottom) were shown. Scale bars, 50 μm. **(F)** Elevated levels of APP/CTFβ and APP/CTFβ after NTI administration. Full-length APP and APP fragments in the hippocampal extracts were shown on western blots. The densitometric analysis of immunoblots was shown. **(G)** Secretase activities in hippocampus of APP/PS transgenic mice. The fluorogenic substrate assay was performed. **(H)** NICD, N-Cad/CTF1 and APLP1-CTF levels in the brains of APP/PS transgenic mice. Immunoprecipitates bound to the specific antibodies recognizing the cytosolic domain of Notch 1 were subjected to western blot. N-Cad/CTF1 and APLP1-CTF were detected using the antibody against C-terminal of N-cadherin and antibody against C-terminal of APLP1, respectively. The representative images (upper) and densitometric analysis of the blots (bottom) were shown. Data are presented as mean ± s.e.m. n = 5-8 per group. (Student's t-test; *P < 0.05, **P < 0.01).

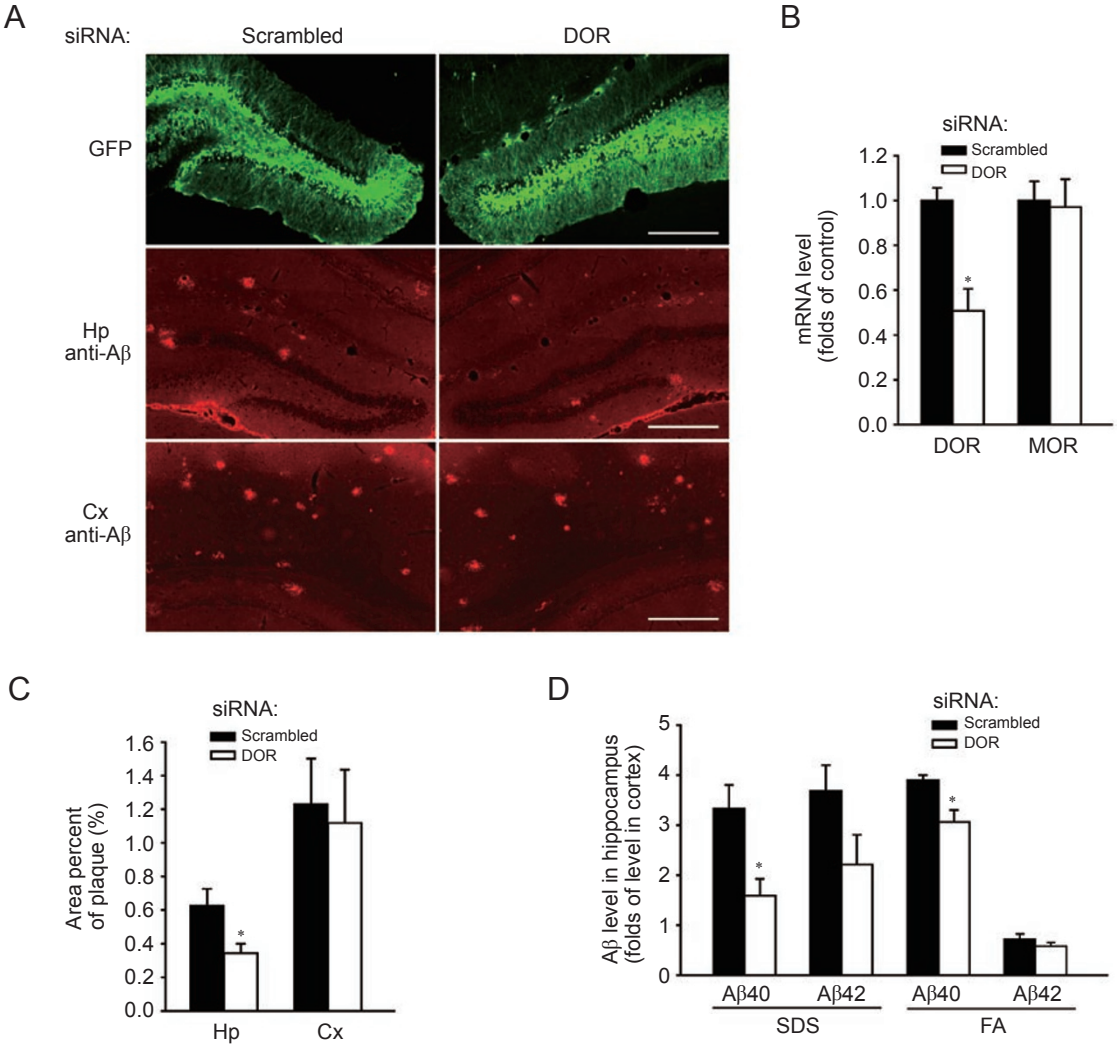

Figure 5 Knockdown of DOR retards Aβ accumulation in mice. **(A)** Knockdown of DOR retards Aβ accumulation and amyloid plaque formation in the hippocampus of TgCRND8 mice. Hippocampi of TgCRND8 mice were bilaterally injected with lentiviral vectors expressing either scrambled siRNA or DOR siRNA, as indicated. At 2 months after injection, brain sections were prepared and subjected to immunofluorescence assay. Representative images of GFP show comparable and consistent expression of lentiviral vectors in the bilateral hippocampus (first row). Amyloid plaques in the bilateral hippocampus (second row) and cortex (third row) were stained using an anti-Aβ antibody 6E10. Scale bars, 200 μm; Hp, hippocampus; Cx, cortex. **(B)** The efficiency of DOR siRNA lentiviral vectors. The mRNA level of DOR as well as that of MOR in hippocampus was determined by quantitative PCR coupled with reverse transcription. n = 6 per group. **(C)** Morphometric analysis of the percent area of the hippocampus (Hp) and cortex (Cx) occupied by 6E10-immunoreactive amyloid plaques (n = 6 per group). **(D)** Hippocampal versus cortical Aβ levels. SDS- or formic acid (FA)-soluble proteins in the hippocampus and cortex were extracted and subjected to ELISA for Aβ (n = 6 per group). Data are presented as mean ± s.e.m. (Student's t-test; $^*P < 0.05$).

with reverse transcription (qRT-PCR) analysis indicated that injection of lenti-siDOR remarkably reduced endogenous DOR expression levels (Figure 5B). As shown in Figure 5A, we observed a significant reduction in 6E10-positive amyloid plaques in the lenti-siDOR-injected hippocampus compared to that in the control vector-injected hippocampus, but not in other brain regions such as the cortex, where no lentiviral vectors were delivered. Morphometric analysis confirmed that knockdown of DOR by lenti-siDOR significantly reduced the formation of amyloid plaques in the hippocampus, whereas in the cortex that received no lentivirus, the amyloid plaque levels are comparable (Figure 5C). ELISA analysis of Aβ levels in the detergent or formic acid extracts from hippocampus and cortex of these mice showed that Aβ40 and Aβ42 were significantly reduced in the hippocampus that

received lenti-siDOR vectors (Figure 5D). These results demonstrate that reduction of the endogenous DOR level leads to a reduction of Aβ and amyloid plaque burden in mouse hippocampus, indicating that DOR contributes to Aβ-dependent pathogenesis *in vivo*.

Discussion

In this study, we report that chronic and systemic treatment of transgenic AD model mice with antagonists of DOR, but not that of MOR, improves cognitive deficits in spatial reference memory and ameliorates major hallmarks of AD, including Aβ pathology, astrogliosis and microgliosis. Our results suggest that the underlying regulatory mechanism is that DOR forms a complex with β- and γ-secretases to mediate the intracellular trafficking of the secretases/GPCR complex into LEL, which contributes to the specific processing of APP to Aβ. On the contrary, activated MOR quickly recycles back to the membrane and has no effect on APP processing. It is also interesting to note that, similar to what we reported previously [23], downstream signaling events, including the G-protein pathway and canonical cAMP pathway, are not involved, as neither blockage of G-protein activation by pertussis toxin nor activation of the cAMP pathway by forskolin or dibutyl-cAMP treatment has detectable effects on secretase activities (data not shown). Importantly, modulation of BACE1 and γ-secretase activities by DOR is substrate specific. Neither activation of DOR *in vitro* nor blockage of DOR *in vivo* affects the processing of Notch, N-cadherin or APLP1 by either β- or γ-secretase. Our study thus provides direct evidence that antagonism of DOR specifically blocks the amyloidogenic pathway and efficaciously prevents AD progression in mice, presenting DOR as a novel potential therapeutic target for specific inhibition of Aβ generation.

In 1980s, there were several double-blinded placebo-controlled clinical studies showing that the nonselective antagonists of opioid receptors, including naloxone and naltrexone, fail to affect overall cognitive functioning in individuals with probable AD [30-32]. However, these studies could not rule out the possibility that selective antagonist of opioid receptors might be efficacious in AD treatment, as DOR, MOR and KOR might play different roles in AD pathology. Very recently, Mucke and co-workers [36] reported that elevation of enkephalin contributes to neuronal and behavioral impairments of AD mice. They also reported that, although administration of β-FNA did not improve the performance of AD model mice in hidden platform testing, as we observed in the present study, β-FNA treatment improved the spatial memory retention, which was not assessed in our water maze testing. They proposed that β-FNA functions downstream of Aβ to reduce memory deficit by counteracting Aβ-induced increase of met-enkephalin signaling. The processing of APP and the Aβ pathogenesis were not investigated in that study. By contrast, our study shows a direct effect of DOR antagonist on Aβ production. Thus, our study, together with other previous works, suggests a complex regulatory role of the opioid signaling system in AD pathology.

Our present study uncovered a molecular mechanism for regulating amyloidogenic APP processing by GPCR-mediated endocytic sorting of BACE1 and γ-secretase in cells. The formation of the receptor/BACE1/γ-secretase complex promotes the sequential proteolysis of APP by these two secretases. Whether the substrate APP is also enriched in the same complex is of interest and is now under further investigation. Thus, either blockage of the association of the receptor with secretases or modulation of the endocytic trafficking of the receptor/BACE1/γ-secretase complex should affect APP processing and the subsequent Aβ-dependent pathogenesis. It is also important to note that fine-tuning of the secretase intracellular trafficking by the receptors also specifically separates proteolysis of APP with that of Notch, N-cadherin and APLP1. Hence, it could be postulated that other membrane GPCRs with similar postendocytic sorting profiles or chemicals modulating the intracellular trafficking of the receptor/secretase complex may regulate APP processing in a similar manner. Given the insidious and progressive nature of AD, a small reduction in Aβ generation would have a profound impact on clinical outcome. Therefore, targeting brain-enriched receptors that form complexes with BACE1 and γ-secretase and mediate endocytic sorting of secretases represents an appealing avenue for the development of new therapeutic strategy against AD with less side effects.

Materials and Methods

APP/PS transgenic mice and drug treatment

APP/PS transgenic mice (Jackson Laboratory, stock number 004462) coexpress a chimeric mouse/human APP containing the K595N/M596L Swedish mutations (APPswe) and a mutant human PS1 with the exon-9 deletion (PS1ΔE9) under the control of mouse prion promoter elements. These mice were maintained as hemizygotes by crossing transgenic mice with B6C3F1/J mice. Offsprings were genotyped with PCR according to a protocol provided by the Jackson Laboratory. Gender- and age-matched 4-month-old APP/PS transgenic mice and their WT littermates were randomly assigned into three groups. They were chronically administrated with NTI (Sigma), β-FNA (Tocris) or vehicle only (water) by gavage once per day until they were 6-months old (n = 8-17 mice per group). NTI and β-FNA were freshly prepared as aqueous solution and the volume for administration was below 400 μl.

At ~6.5 months of age, following assessment of spatial memory functions by the MWM test, mice were anesthetized with 400 mg/kg choloral hydrate (Sigma) and sacrificed by transcardiac perfusion with 0.9% saline. The brains were harvested and cut in half sagittally. One hemisphere was dissected into hippocampus and cortex, rapidly frozen in liquid nitrogen and stored at –80 ºC for biochemical analysis. The other hemisphere was fixed for 6 h in 4% paraformaldehyde and cryoprotected in 30% sucrose. Coronal cryosections (14 μm) were cut.

All mice were given *ad libitum* access to food and water. All experiments were in accordance with the National Institutes of Health Guide for the Care and Use of Laboratory Animals and were approved by the Biological Research Ethics Committee, Shanghai Institutes for biological Sciences, Chinese Academy of Sciences.

TgCRND8 mice, production of siRNA lentiviral vectors and intracerebral injection

The protocols of vector construction and lentiviral vector production have been described previously [64]. The following siRNA oligonucleotides were used: siDOR (5′-GGC CAA GCU GAU CAA UAU A-3′) and scrambled (5′-GCA CGA UAU ACA AGG AUC U-3′). HEK293T cells were transfected with the vector and packaging plasmids, the supernatants were collected and viruses were concentrated by ultracentrifugation. The vectors contained GFP coding sequence, and the concentrated virus stocks were tittered on HEK293T cells based on GFP expression.

TgCRND8 transgenic mice (a kind gift from Dr David Westaway, University of Alberta, USA) express a human APP transgene (APP_{695}) bearing missense mutations that cause AD in humans (K670N, M671L and V717F). These mice were maintained as hemizygotes by crossing transgenic mice to B6C3F1/J mice.

TgCRND8 transgenic mice (3-month-old) were anesthetized with chloral hydrate and placed on stereotaxic apparatus. Lentiviral preparations (2 μl volume, ~2.0×10^6 transducing units per site) were stereotaxically injected into the hippocampus (–2.0 mm anteroposterior from bregma, ±1.5 mm mediolateral from bregma and 2.0 mm below skull surface) with a 5 μl syringe at a speed of 0.5 μl/min. The lentiviral vector targeting DOR was injected into the right hippocampus and that with scrambled sequence into the left. To allow diffusion of the solution into the brain tissue, the needle was left for an additional 5 min before being withdrawn. Mice were then individually housed, allowed to recover from surgery and were sacrificed 2 months after the virus injection.

qRT-PCR

The primer pairs used were mouse DOR sense: 5′-GCT GGT GGA CAT CAA TCG G-3′; antisense: 5′-GCG TAG AGA ACC GGG TTG AG-3′; mouse MOR sense: 5′-TGG CTC CTG GCT CAA CTT G-3′; antisense: 5′-CAG CGT GCT AGT GGC TAA GG-3′; mouse HPRT sense: 5′-CCT GCT GGA TTA CAT TAA AGC ACT G-3′, antisense: 5′-TTC AAC ACT TCG AGA GGT CCT-3′.

Behavioral tests

The details of Morris water maze used in this study have been described previously [65]. Briefly, mice were pretrained for 2 days, with eight trials per day, to find a visible platform 1 cm above the water in a circular pool (1.22 m diameter) filled with water (23 ± 1 ºC). Then, the mice were trained for 6 consecutive days, with four trials per day, to find a platform submerged 1 cm beneath the surface of the water using visual cues followed by a probe trial 24 h after the last training.

Tissue sampling, immunofluorescent and thioflavin S staining

Brian sections were incubated with either anti-Aβ (Covance), anti-GFAP (Zymed), anti-CD11b (BD) primary antibody and then FITC or CY3-conjugated secondary antibody (Jackson). For thioflavin S staining, the sections were incubated with 1% thioflavin S solution for 8 min. Images were acquired using a confocal fluorescence microscope (Leica TCS SP2) and analyzed with Image-Pro Plus 5.1 software (Media Cybernetic). For each mouse, four to five sections were analyzed, and the average was used to calculate group means.

Protein extraction, ELISA and western blots

Hippocampus or cortex tissue was sonicated and lysed in the presence of SDS, and the pellet collected by ultracentrifugation was further extracted in 70% formic acid as described [66]. The level of Aβ40 and Aβ42 was measured by ELISA (Biosource).

Proteins in the SDS extracts were resolved on western blot techniques by anti-N-cadherin (BD), anti-APP-CTF (Sigma), anti-APLP1-CTF (Calbiochem) and anti-Notch (Cell Signaling) antibodies.

In vitro fluorometric secretase activity assay

This assay was performed as reported [67]. In brief, membrane-enriched fraction from cell lysate or tissue homogenate was incubated with 10 μM specific fluorogenic substrate for each secretase (Calbiochem). After incubation, fluorescence was measured using SpectraMax M5 spectrometer (Molecular Devices).

Membrane protein purification

HEK293T cells grown on 6-cm dishes were washed in ice cold PBS (0.1 M sodium phosphate, 0.15 M sodium chloride (pH 8.0)) and incubated for 2 h at 4 ºC in PBS containing 2 mM EZ-link Sulfo-NHS-LC-Biotin (Thermo). Thereafter, biotinylation was quenched by washing three times in PBS containing 100 mM glycine. Then, cells were lysed in RIPA buffer (50 mM HEPES (pH 7.5), 150 mM NaCl, 10% glycerol and 1% Triton) for 1 h at 4 ºC. Biotinylated proteins were precipitated with streptavidin-sepharose and detected by immunoblot.

Immunoprecipitation

Cells were lysed and immunoprecipitated with FLAG-specific M2 beads (Sigma) in the buffer containing 50 mM HEPES (pH 7.5), 150 mM NaCl, 10% glycerol, 0.5 mg/ml BSA, 0.2% Triton X-100 and cocktail protease inhibitors (Roche). The immunoprecipitated complexes and cell lysates were separated by SDS-PAGE and blotted with the indicated antibodies. For the double immunoprecipitation, the conditions were the same except that the first-run immunoprecipitates with FLAG-beads were eluted by incubation with 0.3 mg/ml FLAG peptide for 30 min and then the elution was carried out for the second-run immunoprecipitation using HA-beads.

Confocal fluorescence time-lapse microscopy

HEK293T cells were cultured on 35-mm glass bottom culture

dishes and co-transfected with RFP-BACE1, GFP-PS1 and HA-tagged DOR. Time-lapse experiment was done 42 h after transfection using a Ultraview laser spinning disc confocal microscope (Perkin Elmer) with a 60 × 1.4 N.A. objective. Images were acquired using Ultraview software (PerkinElmer) at 3-s intervals at 37 ºC.

Statistics

Behavior scores during Morris water maze were analyzed using two-way repeated measures analysis of variance (two-way RMANOVA), with treatment group and training block as sources of variation (SigmaStat 3.5 software). Tukey's *post hoc* tests were used to determine individual differences in groups with respect to vehicle-treated APP/PS transgenic mice or WT mice. All the other *in vitro* and *in vivo* data were analyzed by Student's *t*-test.

Acknowledgments

We thank Dr David Westaway (University of Alberta) for TgCRND8 mice, Dr David Baltimore (California Institute of Technology) for lentiviral constructs, Dr Raphael Kopan (Washington University) for the plasmid of myc-tagged NotchΔE and Dr Johan Lundkvist (Karolinska Institutet) for the plasmid of Gal4-driven luciferase reporter gene, the plasmid of APP/CTFβ-GVP and NΔE-GVP. We appreciate Shunmei Xin, Shan Chen and Xianglu Zeng for their technical assistance. We thank all members of the lab for sharing reagents and advice. This research was supported by the Ministry of Science and Technology (2009ZX09103-684), the National Natural Science Foundation of China (30621091, 30625014, 30623003, 30871285 and 90713047), the Shanghai Municipal Commission for Science and Technology (07PJ14099 and 09JC1416400), and the Chinese Academy of Sciences (2007KIP204).

References

1 Albert MS. Cognitive and neurobiologic markers of early Alzheimer disease. *Proc Natl Acad Sci USA* 1996; **93**:13547-13551.
2 Selkoe DJ. Alzheimer's disease: genotypes, phenotypes, and treatments. *Science* 1997; **275**:630-631.
3 Selkoe DJ. Deciphering the genesis and fate of amyloid β-protein yields novel therapies for Alzheimer disease. *J Clin Invest* 2002; **110**:1375-1381.
4 Hardy J, Selkoe DJ. The amyloid hypothesis of Alzheimer's disease: progress and problems on the road to therapeutics. *Science* 2002; **297**:353-356.
5 Selkoe DJ. Clearing the brain's amyloid cobwebs. *Neuron* 2001; **32**:177-180.
6 Kang J, Lemaire HG, Unterbeck A, *et al*. The precursor of Alzheimer's disease amyloid A4 protein resembles a cell-surface receptor. *Nature* 1987; **325**:733-736.
7 Sinha S, Anderson JP, Barbour R, *et al*. Purification and cloning of amyloid precursor protein β-secretase from human brain. *Nature* 1999; **402**:537-540.
8 Takasugi N, Tomita T, Hayashi I, *et al*. The role of presenilin cofactors in the gamma-secretase complex. *Nature* 2003; **422**:438-441.
9 Vassar R, Bennett BD, Babu-Khan S, *et al*. Beta-secretase cleavage of Alzheimer's amyloid precursor protein by the transmembrane aspartic protease BACE. *Science* 1999; **286**:735-741.
10 Sinha S, Lieberburg I. Cellular mechanisms of beta-amyloid production and secretion. *Proc Natl Acad Sci USA* 1999; **96**:11049-11053.
11 De Strooper B. Aph-1, Pen-2, and Nicastrin with Presenilin generate an active gamma-secretase complex. *Neuron* 2003; **38**:9-12.
12 Lichtenthaler SF, Wang R, Grimm H, Uljon SN, Masters CL, Beyreuther K. Mechanism of the cleavage specificity of Alzheimer's disease γ-secretase identified by phenylalanine-scanning mutagenesis of the transmembrane domain of the amyloid precursor protein. *Proc Natl Acad Sci USA* 1999; **96**:3053-3058.
13 Ling Y, Morgan K, Kalsheker N. Amyloid precursor protein (APP) and the biology of proteolytic processing: relevance to Alzheimer's disease. *Int J Biochem Cell Biol* 2003; **35**:1505-1535.
14 Iwata N, Tsubuki S, Takaki Y, *et al*. Metabolic regulation of brain Abeta by neprilysin. *Science* 2001; **292**:1550-1552.
15 Farris W, Mansourian S, Chang Y, *et al*. Insulin-degrading enzyme regulates the levels of insulin, amyloid β-protein, and the β-amyloid precursor protein intracellular domain *in vivo*. *Proc Natl Acad Sci USA* 2003; **100**:4162-4167.
16 Eckman EA, Watson M, Marlow L, Sambamurti K, Eckman CB. Alzheimer's disease β-amyloid peptide is increased in mice deficient in endothelin-converting enzyme. *J Biol Chem* 2003; **278**:2081-2084.
17 Hemming ML, Selkoe DJ. Amyloid β-protein is degraded by cellular angiotensin-converting enzyme (ACE) and elevated by an ACE inhibitor. *J Biol Chem* 2005; **280**:37644-37650.
18 Blennow K, de Leon MJ, Zetterberg H. Alzheimer's disease. *Lancet* 2006; **368**:387-403.
19 Nitsch RM, Slack BE, Wurtman RJ, Growdon JH. Release of Alzheimer amyloid precursor derivatives stimulated by activation of muscarinic acetylcholine receptors. *Science* 1992; **258**:304-307.
20 Xu H, Gouras GK, Greenfield JP, *et al*. Estrogen reduces neuronal generation of Alzheimer β-amyloid peptides. *Nat Med* 1998; **4**:447-451.
21 Weggen S, Eriksen JL, Das P, *et al*. A subset of NSAIDs lower amyloidogenic Aβ42 independently of cyclooxygenase activity. *Nature* 2001; **414**:212-216.
22 Cai D, Netzer WJ, Zhong M, *et al*. Presenilin-1 uses phospholipase D1 as a negative regulator of β-amyloid formation. *Proc Natl Acad Sci USA* 2006; **103**:1941-1946.
23 Ni Y, Zhao, X, Bao G, *et al*. Activation of β2-adrenergic receptor stimulates γ-secretase activity and accelerates amyloid plaque formation. *Nat Med* 2006; **12**:1390-1396.
24 Thathiah A, Spittaels K, Hoffmann M, *et al*. The orphan G protein-coupled receptor 3 modulates amyloid-β peptide generation in neurons. *Science* 2009; **323**:946-951.
25 Bramham CR, Milgram NW, Srebro B. Delta opioid receptor activation is required to induce LTP of synaptic transmission in the lateral perforant path *in vivo*. *Brain Res* 1991; **567**:42-50.
26 Wagner JJ, Terman GW, Chavkin C. Endogenous dynorphins inhibit excitatory neurotransmission and block LTP induction

in the hippocampus. *Nature* 1993; **363**:451-454.
27 Gallagher M, King RA, Young NB. Opiate antagonists improve spatial memory. *Science* 1983; **221**:975-976.
28 Izquierdo I, Paiva AC, Elisabetsky E. Post-training intraperitoneal administration of leu-enkephalin and β-endorphin causes retrograde amnesia for two different tasks in rats. *Behav Neural Biol* 1980; **28**:246-250.
29 Reisberg B, Ferris SH, Anand R, *et al*. Effects of naloxone in senile dementia: a double-blind trial. *N Engl J Med* 1983; **308**:721-722.
30 Tariot PN, Sunderland T, Murphy DL, *et al*. Design and interpretation of opiate antagonist trials in dementia. *Prog Neuropsychopharmacol Biol Psychiatry* 1986; **10**:611-626.
31 Pomara N, Roberts R, Rhiew HB, Stanley M, Gershon S. Multiple, single-dose naltrexone administrations fail to effect overall cognitive functioning and plasma cortisol in individuals with probable Alzheimer's disease. *Neurobiol Aging* 1985; **6**:233-236.
32 Serby M, Resnick R, Jordan B, Adler J, Corwin J, Rotrosen JP. Naltrexone and Alzheimer's disease. *Prog Neuropsychopharmacol Biol Psychiatry* 1986; **10**:587-590.
33 Kieffer BL, Gaveriaux-Ruff C. Exploring the opioid system by gene knockout. *Prog Neurobiol* 2002; **66**:285-306.
34 Mathieu-Kia AM, Fan LQ, Kreek MJ, Simon EJ, Hiller JM. Mu-, delta- and κ-opioid receptor populations are differentially altered in distinct areas of postmortem brains of Alzheimer's disease patients. *Brain Res* 2001; **893**:121-134.
35 Risser D, You ZB, Cairns N, *et al*. Endogenous opioids in frontal cortex of patients with Down syndrome. *Neurosci Lett* 1996; **203**:111-114.
36 Meilandt WJ, Yu GQ, Chin J, *et al*. Enkephalin elevations contribute to neuronal and behavioral impairments in a transgenic mouse model of Alzheimer's disease. *J Neurosci* 2008; **28**:5007-5017.
37 Marks N, Berg MJ. Neurosecretases provide strategies to treat sporadic and familial Alzheimer disorders. *Neurochem Int* 2008; **52**:184-215.
38 Schroeter EH, Kisslinger JA, Kopan R. Notch-1 signalling requires ligand-induced proteolytic release of intracellular domain. *Nature* 1998; **393**:382-386.
39 Karlstrom H, Bergman A, Lendahl U, Naslund J, Lundkvist J. A sensitive and quantitative assay for measuring cleavage of presenilin substrates. *J Biol Chem* 2002; **277**:6763-6766.
40 Allen JA, Halverson-Tamboli RA, Rasenick MM. Lipid raft microdomains and neurotransmitter signalling. *Nat Rev Neurosci* 2007; **8**:128-140.
41 Sargiacomo M, Lisanti M, Graeve L, Le Bivic A, Rodriguez-Boulan E. Integral and peripheral protein composition of the apical and basolateral membrane domains in MDCK cells. *J Membr Biol* 1989; **107**:277-286.
42 von Arnim CA, Tangredi MM, Peltan ID, *et al*. Demonstration of BACE (β-secretase) phosphorylation and its interaction with GGA1 in cells by fluorescence-lifetime imaging microscopy. *J Cell Sci* 2004; **117**:5437-5445.
43 Kaether C, Lammich S, Edbauer D, *et al*. Presenilin-1 affects trafficking and processing of βAPP and is targeted in a complex with nicastrin to the plasma membrane. *J Cell Biol* 2002; **158**:551-561.
44 Whistler JL, Enquist J, Marley A, *et al*. Modulation of postendocytic sorting of G protein-coupled receptors. *Science* 2002; **297**:615-620.
45 Finn AK, Whistler JL. Endocytosis of the mu opioid receptor reduces tolerance and a cellular hallmark of opiate withdrawal. *Neuron* 2001; **32**:829-839.
46 Afify EA, Law PY, Riedl M, Elde R, Loh HH. Role of carboxyl terminus of mu-and δ-opioid receptor in agonist-induced down-regulation. *Brain Res Mol Brain Res* 1998; **54**:24-34.
47 Portoghese PS, Sultana M, Takemori AE. Naltrindole, a highly selective and potent non-peptide δ opioid receptor antagonist. *Eur J Pharmacol* 1988; **146**:185-186.
48 Ward SJ, Portoghese PS, Takemori AE. Pharmacological characterization *in vivo* of the novel opiate, β-funaltrexamine. *J Pharmacol Exp Ther* 1982; **220**:494-498.
49 Waldhoer M, Bartlett SE, Whistler JL. Opioid receptors. *Annu Rev Biochem* 2004; **73**:953-990.
50 Dhawan BN, Cesselin F, Raghubir R, *et al*. International Union of Pharmacology. XII. Classification of opioid receptors. *Pharmacol Rev* 1996; **48**:567-592.
51 Fernandez B, Antelo MT, Kitchen I, Viveros MP. Effects of neonatal naltrindole treatment on antinociceptive and behavioral responses to mu and kappa agonists in rats. *Pharmacol Biochem Behav* 1999; **62**:145-149.
52 Jankowsky JL, Slunt HH, Ratovitski T, Jenkins NA, Copeland NG, Borchelt DR. Co-expression of multiple transgenes in mouse CNS: a comparison of strategies. *Biomol Eng* 2001; **17**:157-165.
53 Garcia-Alloza M, Robbins EM, Zhang-Nunes SX, *et al*. Characterization of amyloid deposition in the APPswe/PS1dE9 mouse model of Alzheimer disease. *Neurobiol Dis* 2006; **24**:516-524.
54 Reiserer RS, Harrison FE, Syverud DC, McDonald MP. Impaired spatial learning in the APPSwe + PSEN1ΔE9 bigenic mouse model of Alzheimer's disease. *Genes Brain Behav* 2007; **6**:54-65.
55 Kitchen I, Pinker SR. Antagonism of swim-stress-induced antinociception by the δ-opioid receptor antagonist naltrindole in adult and young rats. *Br J Pharmacol* 1990; **100**:685-688.
56 Berrendero F, Maldonado R. Involvement of the opioid system in the anxiolytic-like effects induced by δ(9)-tetrahydrocannabinol. *Psychopharmacology (Berl)* 2002; **163**:111-117.
57 Matsuzawa S, Suzuki T, Misawa M, Nagase H. Involvement of mu- and δ-opioid receptors in the ethanol-associated place preference in rats exposed to foot shock stress. *Brain Res* 1998; **803**:169-177.
58 Negus SS, Henriksen SJ, Mattox A, *et al*. Effect of antagonists selective for mu, δ and κ opioid receptors on the reinforcing effects of heroin in rats. *J Pharmacol Exp Ther* 1993; **265**:1245-1252.
59 Cao D, Lu H, Lewis TL, Li L. Intake of sucrose-sweetened water induces insulin resistance and exacerbates memory deficits and amyloidosis in a transgenic mouse model of Alzheimer disease. *J Biol Chem* 2007; **282**:36275-6282.
60 McGeer PL, Itagaki S, Tago H, McGeer EG. Reactive microglia in patients with senile dementia of the Alzheimer type are positive for the histocompatibility glycoprotein HLA-DR. *Neurosci Lett* 1987; **79**:195-200.
61 Simard AR, Soulet D, Gowing G, Julien JP, Rivest S. Bone

marrow-derived microglia play a critical role in restricting senile plaque formation in Alzheimer's disease. *Neuron* 2006; **49**:489-502.

62 Eggert S, Paliga K, Soba P, *et al*. The proteolytic processing of the amyloid precursor protein gene family members APLP-1 and APLP-2 involves α-, β-, γ-, and epsilon-like cleavages: modulation of APLP-1 processing by N-glycosylation. *J Biol Chem* 2004; **279**:18146-18156.

63 Chishti MA, Yang DS, Janus C, *et al*. Early-onset amyloid deposition and cognitive deficits in transgenic mice expressing a double mutant form of amyloid precursor protein 695. *J Biol Chem* 2001; **276**:21562-21570.

64 Qin XF, An DS, Chen IS, Baltimore D. Inhibiting HIV-1 infection in human T cells by lentiviral-mediated delivery of small interfering RNA against CCR5. *Proc Natl Acad Sci USA* 2003; **100**:183-188.

65 Westerman MA, Cooper-Blacketer D, Mariash A, *et al*. The relationship between Aβ and memory in the Tg2576 mouse model of Alzheimer's disease. *J Neurosci* 2002; **22**:1858-1867.

66 Lazarov O, Robinson J, Tang YP, *et al*. Environmental enrichment reduces Aβ levels and amyloid deposition in transgenic mice. *Cell* 2005; **120**:701-713.

67 Farmery MR, Tjernberg LO, Pursglove SE, Bergman A, Winblad B, Naslund J. Partial purification and characterization of γ-secretase from post-mortem human brain. *J Biol Chem* 2003; **278**:24277-24284.

(**Supplementary information** is linked to the online version of the paper on the *Cell Research* website.)